The Laryngoscope

Biomechanical Evaluation of Human and Porcine Auricular Cartilage

David A. Zopf, MD, MS; Colleen L. Flanagan, MSE; Hassan B. Nasser, BS; Anna G. Mitsak, PhD; Farhan S. Huq, MD, MS; Vishnu Rajendran; Glenn E. Green, MD; Scott J. Hollister, PhD

Objectives/Hypothesis: The mechanical properties of normal auricular cartilage provide a benchmark against which to characterize changes in auricular structure/function due to genetic defects creating phenotypic abnormalities in collagen subtypes. Such properties also provide inputs/targets for auricular reconstruction scaffold design. Several studies report the biomechanical properties for septal, costal, and articular cartilage. However, analogous data for auricular cartilage are lacking. Therefore, our aim in this study was to characterize both whole-ear and auricular cartilage mechanics by mechanically testing specimens and fitting the results to nonlinear constitutive models.

Study Design: Mechanical testing of whole ears and auricular cartilage punch biopsies.

Methods: Whole human cadaveric ear and auricular cartilage punch biopsies from both porcine and human cartilage were subjected to whole-ear helix-down compression and quasistatic unconfined compression tests. Common hyperelastic constitutive laws (widely used to characterize soft tissue mechanics) were evaluated for their ability to represent the stress-strain behavior of auricular cartilage.

Results: Load displacement curves for whole ear testing exhibited compliant linear behavior until after significant displacement where nonlinear stiffening occurred. All five commonly used two-term hyperelastic soft tissue constitutive models successfully fit both human and porcine nonlinear elastic behavior (mean R^2 fit >0.95).

Conclusions: Auricular cartilage exhibits nonlinear strain-stiffening elastic behavior that is similar to other soft tissues in the body. The whole ear exhibits compliant behavior with strain stiffening at high displacement. The constants from the hyperelastic model fits provide quantitative baselines for both human and porcine (a commonly used animal model for auricular tissue engineering) auricular mechanics.

Key Words: Auricular cartilage, biomechanics, auricular tissue engineering, cartilage computational modeling, nonlinear elasticity.

Level of Evidence: NA

***Laryngoscope*, 125:E262–E268, 2015**

INTRODUCTION

The external ear, or auricle, has aesthetic significance and serves as a reverberation chamber to amplify and filter sound waves. It permits directionality and preferentially selects sounds in the human speech frequency range, while channeling them to the external auditory canal and the tympanic membrane.[1] The auricle has a layered structure and is composed of three principal components—skin, perichondrium, and auricular cartilage. The perichondrium is tightly bound to the cartilage on its lateral surface and more loosely bound to its medial surface.[2] Auricular cartilage provides mechanical support to the ear and also determines the external ear's characteristic shape.

Pathology involving auricular cartilage is most commonly due to congenital malformations or acquired causes, such as neoplasms or trauma. Genetic defects involving mutations of collagen subtypes, such as Alport syndrome, osteogenesis imperfecta I, and spondyloepiphyseal dysplasia, can result in syndromes with complex phenotypes comprised of hearing loss and abnormalities or absence of the external cartilaginous structures.[3–5] Approaches to the repair of auricular cartilage defects have historically focused on autologous cartilage grafting and alloplastic material implants.[6–8] However, these approaches have pronounced drawbacks. Some include risk of chronic infection, implant migration and erosion, and increased donor site morbidity associated with the multiple operative procedures often required for surgical reconstruction. It is likely that erosion and implant migration are related in part to the alloplastic material mechanical stiffness being much greater than native auricular cartilage mechanical stiffness. More recently, attempts to tissue-engineer auricular constructs have

From the Department of Otolaryngology–Head and Neck Surgery (D.A.Z., H.B.N., F.S.H., G.E.G.), Division of Pediatric Otolaryngology, University of Michigan Medical School, Ann Arbor, Michigan; and the Department of Biomedical Engineering (C.L.F., A.G.M., V.R., S.J.H.), Department of Mechanical Engineering (S.J.H.) and Department of Surgery (S.J.H.), University of Michigan, Ann Arbor, Michigan, U.S.A.

Editor's Note: This Manuscript was accepted for publication October 28, 2014.

The authors have no other funding, financial relationships, or conflicts of interest to disclose.

This work was supported by a Michigan Institute for Clinical & Health Research grant. H.B.N. is supported by a T32 DC005356 training grant.

Send correspondence to Dr. Scott J. Hollister, Department of Biomedical Engineering, University of Michigan, Lurie Biomedical Engineering Bldg. Rm 2208, 1101 Beal Ave., Ann Arbor, MI 48109-2110. E-mail: scottho@umich.edu

DOI: 10.1002/lary.25040

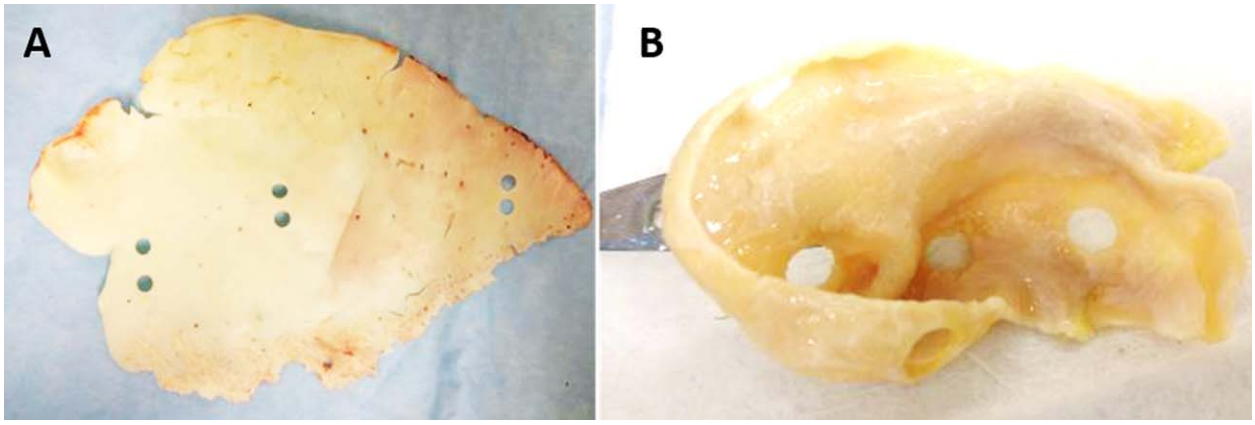

Fig. 1. Punch biopsies of porcine and human auricular cartilage. (A) Two punch biopsies were taken from each pig ear (n = 8) at a proximal (adjacent to mastoid), mid, and distal site. (B) Following the whole-ear helix-down compression test, single biopsies were taken from each human ear (n = 5) from five standardized locations: root of the helix, posterosuperior helix, triangular fossa, conchal bowl, and tragus to assess for regional differences in the complex confirmation of the auricle.

been undertaken with the hope of reducing the donor site morbidity and complications associated with surgical reconstruction, as well as offering patients an improved functional and aesthetic result.[9–11]

As discussed in a recent review of efforts in tissue-engineering auricular cartilage,[12] a principal challenge in engineering cartilage for ear reconstruction is ensuring mechanical competency of constructs, a task that largely relies on the ability of engineered cartilage to mimic the biomechanical properties of native tissue. As highlighted by Nimeskern et al.,[12] although a number of studies have reported some functional evaluation of tissue-engineered auricular constructs,[13–16] optimal construct design is limited by the lack of an adequate benchmark detailing the mechanical properties of native tissue.

Despite the obvious need for robust information on the mechanical properties of native auricular cartilage, the auricular cartilage biomechanics literature is sparse.[17–19] In contrast, the mechanical properties of articular, septal, and costal native cartilage and tissue-engineered constructs are thoroughly studied and well characterized using mathematical constitutive models.[11,13,20–27] Mathematical constitutive modeling offers the ability to quantitatively characterize normal auricular cartilage behavior for comparison to auricular cartilage with phenotypic abnormalities as well as provide quantitative input for tissue-engineered construct design.

The goals of the present study were to 1) determine mechanical properties of whole human ears as well as porcine and human auricular cartilage via biomechanical testing and 2) evaluate the use of common hyperelastic constitutive models for predicting the mechanical behavior of auricular cartilage under compressive loading. Defining robust biomechanical data for porcine and human auricular cartilage may serve as a reference when studying genetically defective collagen subtypes as well as a benchmark for designing tissue-engineered auricular constructs.

MATERIALS AND METHODS

Human and Porcine Auricular Cartilage

All animal tissue samples were acquired in accordance with the guidelines set by the Institutional Animal Care and Use Committee at the University of Michigan Medical School. Auricular cartilage specimens were harvested from fresh porcine ears. Porcine auricular cartilage was harvested from eight adult pigs and kept in lactated Ringer's solution until testing, which was performed within 6 hours of harvest. Cartilage was freed from surrounding perichondrium and connective tissue. For porcine cartilage, two 6-mm-diameter punch biopsies were taken from each ear at a proximal (adjacent to mastoid), mid, and distal site along the cartilaginous framework, and wet weight was determined (Fig. 1A). After mechanical testing was completed, punch biopsy specimen dry weights were determined after lyophilization, and the water content of each specimen was calculated (n = 3 animals).

A total of nine fresh human auricles from seven donors (age range, 46–94 years; mean age, 72.6 ± 17 years; 3 males/4 females) were obtained 48 to 72 hours postmortem. Auricular cartilage was freed from surrounding perichondrium and connective tissue and kept moist with lactated Ringer's solution. The ear was then subjected to a whole-ear helix-down compression test, as described below. Following this first test, 6-mm-diameter punch biopsies were taken from each human specimen. To assess for regional differences in the complex confirmation of the human auricle, punch biopsies were taken from each ear from the following five standardized locations: root of the helix, posterosuperior helix, triangular fossa, conchal bowl, and tragus (Fig. 1B). Wet weight was obtained (n = 3 donors). All test measurements were obtained directly after specimen withdrawal from lactated Ringer's solution. Following completion of mechanical testing, biopsy specimens were lyophilized and dry weights were determined. Last, water content was calculated.

Biomechanical Testing

Using a method previously unreported in the literature, human ears were dissected free of perichondrium and first subjected to a whole-ear helix-down unconfined compression test to determine whole-ear stiffness. Fixed compression platens were used to apply load at a constant displacement rate of 10 mm/

Fig. 2. The MTS Alliance RT/30 machine setup. Whole human cadaveric ears were subjected to a whole-ear helix-down compression test.

min. A preload of 0.01 pounds was applied to define the start of the test and the specimen height in the helix-down position. Stiffness, the slope of the load displacement curve, was calculated in the linear region between 2 and 4 mm of displacement. Following this test, biopsies were taken from each ear and sequentially subjected to a 10% strain-stress relaxation test in confined compression (data not reported here). Specimens were allowed to recover overnight in lactated Ringer's solution at 4°C. Once specimens were equilibrated to room temperature, an unconfined compression test to 60% strain was performed at a displacement rate of 300 μm/second. All mechanical tests were performed using an MTS Alliance RT/30 (MTS Systems Corp., Eden Prairie, MN) testing machine with a 500N load cell (Fig. 2). Porcine punch biopsy specimens were subjected to the same testing methodology as the human specimens (excluding the whole-ear helix-down compression test due to the flat nature of the porcine auricle).

Hyperelastic Model Fitting

Auricular cartilage exhibits complex mechanical behavior. At a minimum, auricular cartilage may be characterized as a hyperelastic material (a special case of a nonlinear elastic material), in which stress nonlinearly increases with strain, similar to most soft tissues in the body.[27–30] Unlike the unique representation of linear elasticity using Hooke's law, however, there is no unique model that represents hyperelastic stress-strain behavior. We have chosen to utilize and compare five different hyperelastic constitutive models developed by Ogden,[31] Fung/Kenedi,[32] Yeoh,[33] Mooney-Rivlin,[34,35] and Arruda-Boyce.[36] These models are widely used to model nonlinear soft tissue mechanics and are utilized in commercial finite element programs. Although many of these models allow a large number of parameters, we have restricted each model to two parameters to determine the simplest form for modeling auricular cartilage behavior similar to an approach used by Brown et al.[27] for modeling human articular cartilage.

All elastic materials, linear or nonlinear, may be represented by a strain energy function, denoted as W. This strain energy function depends on model parameters and a measure of deformation. The model parameters are fit to data using curve-fitting optimization methods. The measure of deformation may include strain, specialized deformation tensors, or stretch ratios. We have chosen stretch ratios, which are simply the ratios of the specimen length after deformation divided by the specimen length before deformation. Note that the term *stretch ratio*, denoted by λ, is defined for both compression ($0<\lambda<1$) and tension ($1<\lambda<\infty$), although for the experimental compression data presented here λ will always be in the range $0.35<\lambda<1$. Denoting the two model parameters as a and b, the strain energy functions W can be written for each model as follows:

$$\text{Ogden}: W=\frac{a}{b}\left(\lambda_1^b+\lambda_2^b+\lambda_3^b-3\right) \tag{1}$$

$$\text{Fung/Kenedi}: W=a\left[e^{\frac{b}{2}\left(\lambda_3^2-1\right)}\right]-a \tag{2}$$

$$\text{Yeoh}: W=a\left(\lambda_1^2+\lambda_2^2+\lambda_3^2-3\right)+b\left(\lambda_1^2+\lambda_2^2+\lambda_3^2-3\right)^2 \tag{3}$$

$$\text{Mooney-Rivlin}: W=a\left(\lambda_1^2+\lambda_2^2+\lambda_3^2-3\right)+b\left(\lambda_1^2\lambda_2^2+\lambda_1^2\lambda_3^2+\lambda_2^2\lambda_3^2-3\right) \tag{4}$$

$$\text{Arruda-Boyce}: W=a\left[\frac{1}{2}\left(\lambda_1^2+\lambda_2^2+\lambda_3^2-3\right)+\frac{1}{20b^2}\left(\lambda_1^4+\lambda_2^4+\lambda_3^4+2\lambda_1^2\lambda_2^2+2\lambda_1^2\lambda_3^2+2\lambda_2^2\lambda_3^2-9\right)\right] \tag{5}$$

Note that although the Fung/Kenedi model is explicitly one dimensional, the other models are written in terms of three dimensions with three stretch ratios λ_1, λ_2, and λ_3 in each of the three directions. Given that we assume the auricular cartilage is incompressible (i.e., the volume does not change during deformation although the shape does) with $\lambda_1\lambda_2\lambda_3=1$, and we further assume that the transverse stretch ratios are equal $\lambda_1=\lambda_2$, we can generate all models in terms of λ_3 alone. Once this is done, we can then calculate the final stress versus stretch relationship from the following general continuum mechanics equation for an incompressible material:

$$T_{33}=-\frac{1}{\lambda_3}p+\frac{\partial W}{\partial \lambda_3} \tag{6}$$

Where T_{33} is the uniaxial first Piola-Kirchoff stress component (defined as force divided by the original area of the specimen), p is the hydrostatic pressure, W is one of the five strain energy functions from Equations (1) to 5, and λ_3 is the stretch ratio in the compression direction. We solve for p using the fact that stress is applied to only one face of the specimen. Once p is determined and the derivative in Equation (6) is calculated, we then have a value for T_{33} in terms of a, b, and λ_3. A Microsoft Excel (Microsoft Corp., Redmond, WA) data file is generated from the experimental compression testing with experimental values of T_{33} and λ_3. The model parameters a and b are then fit to this experimental data by minimizing the difference between $T_{33}^{\text{experiment}}$ and T_{33}^{model} in a least squares sense:

$$\underset{a,b}{Min}\left(T_{33}^{\text{experimental}}-T_{33}^{\text{model}}\right)^2 \tag{7}$$

The least squares optimization was performed using the fmincon and fminunc routines from MATLAB (MathWorks, Natick, MA). This fitting was done for 24 human auricular cartilage specimens from a total of five individual donors and 30 porcine auricular cartilage specimens for all five hyperelastic models. Goodness of fit was characterized by calculating the coefficient of determination R^2, for which a value >0.95 is considered a good fit.[30]

TABLE I.
Mean Wet/Dry Weights and Calculated Water Content for Porcine (n = 3 Animal) and Human (n = 3 Donors) Auricular Punch Biopsies.

Site	Wet Weight (mg)	Dry Weight (mg)	Water Content (%)
Porcine			
Proximal	66.3 ± 9.6	19.2 ± 2.3	70.9 ± 1.9
Mid	51.2 ± 8.4	14.7 ± 3.4	71.6 ± 2.7
Distal	30.3 ± 8.0	8.7 ± 2.4	71.4 ± 2.0
Human			
Tragal	35.0 ± 3.6	9.3 ± 5.6	73.3 ± 5.6
Root of helix	32.3 ± 3.8	9.3 ± 3.2	71.1 ± 3.2
Posterosuperior helix	35.0 ± 7.2	9.3 ± 2.7	73.3 ± 2.7
Triangular fossa	38.0 ± 3.6	10.0 ± 2.6	73.7 ± 2.6
Concha	44.33 ± 13.6	11.0 ± 1.8	75.2 ± 1.8

RESULTS

Mean wet and dry weights for porcine and human auricular punch biopsies are presented in Table I. Mean water content ranged from 70.9% to 71.6%, and 71.1% to 75.2% for porcine and human samples, respectively. The whole-ear helix-down compression test was used to evaluate the stiffness and flexibility of whole human ear cartilage. Compression tests of punch biopsy specimens were completed to assess local tissue mechanical properties. Load displacement curves for whole-ear helix-down testing are presented in Figure 3. The helix-down compression test demonstrated a mean geometric stiffness of 0.194 ± 0.202 N/mm.

Experimental results from the unconfined compression test (up to 60% strain) data for porcine and human auricular cartilage were used for the determination of the a and b material coefficients for each hyperelastic model. All hyperelastic constitutive models met the criteria ($R^2 > 0.95$; Table II) for accurately modeling the nonlinear behavior of auricular cartilage, but the Yeoh, Fung/Kenedi, and Mooney-Rivlin models provided more consistent fits for characterizing auricular cartilage mechanics. The Yeoh and Mooney-Rivlin constitutive models can be readily selected for use with commercially available finite element analysis packages. Figure 4 demonstrates the fits for the Fung/Kenedi, Yeoh, and Mooney-Rivlin models for one human ear specimen.

DISCUSSION

This study aimed to characterize the nonlinear mechanical properties of porcine and human auricular cartilage and evaluate the utility of common hyperelastic constitutive models in representing the stress-strain behavior of auricular cartilage. Because porcine-derived cells and porcine in general are widely used as preclinical models for human tissue engineering, biomechanical data for porcine auricular cartilage are presented alongside human data. Porcine and human auricular cartilage specimens were subjected to confined and unconfined compression tests to evaluate stress-strain behavior of these tissues. We demonstrated that auricular cartilage from both porcine and human specimens behaves as a nonlinear hyperelastic material. The nonlinear strain-stiffening behavior of porcine and human auricular cartilage was slightly different, as seen from the nonlinear elastic fits, especially the Fung/Kenedi model. Porcine auricular cartilage was much more compliant than human auricular cartilage under small deformations, as seen by the fact that the a parameter in the Fung/Kenedi model, which is related to the initial stiffness, is much smaller for the porcine specimens than the human specimens. However, the b coefficient in the Fung/Kenedi model is similar between the porcine and human specimens, indicating that porcine and human specimens have similar nonlinear stiffening behaviors.

The five hyperelastic constitutive models we evaluated were judged based on their respective goodness of fit to the experimental data. Of the five analyzed models, all had good mean correlations (>0.95) between experimental and theoretical data, indicating all could accurately represent the nonlinear behavior of both

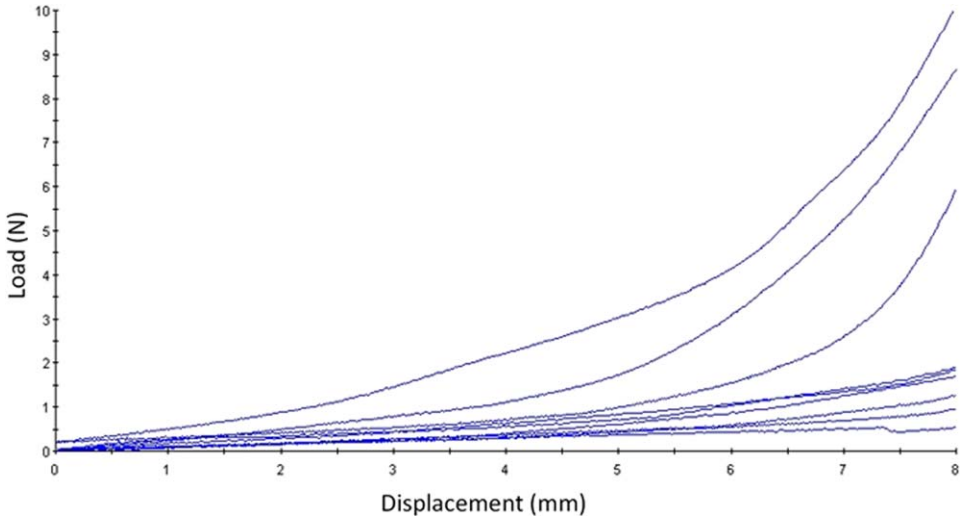

Fig. 3. Whole-ear helix-down load-displacement curve demonstrating nonlinear stiffening behavior for human ear specimens (n = 9).

TABLE II.
Human and Porcine Mean, Standard Deviation, and Range Values of *a* and *b* Parameters for All Five Hyperlastic Constitutive Models.

Model	Specimen	*a* = Mean ± SD	*a* Min/Max	*b* = Mean ± SD	*b* Min/Max	R^2 Mean ± SD	R^2 Min/Max
Ogden	Human	2.45 ± 1.93	0.49/7.46	0.56 ± 0.34	0.14/1.14	0.982 ± 0.13	0.943/0.995
Fung/Kenedi	Human	0.12 ± 0.08	0.02/0.48	8.5 ± 1.62	5.76/11.6	0.996 ± 0.003	0.989/0.999
Arruda	Human	0.42 ± 1.4	0.14/0.71	1,940 ± 1,495	713/8,512	0.975 ± 0.0010	0.950/0.988
Yeoh	Human	0.27 ± 0.11	0.09/0.5	−0.02 ± 0.03	−0.08/0.01	0.989 ± 0.005	0.977/0.997
Mooney-Rivlin	Human	0.30 ± 0.15	0.10/0.62	−0.03 ± 0.05	−0.14/0.03	0.988 ± 0.005	0.975/0.996
Ogden	Porcine	1.65 ± 1.58	0.17/5.03	0.43 ± 0.35	0.06/1.0	0.973 ± 0.018	0.917/0.995
Fung/Kenedi	Porcine	0.04 ± 0.03	0.01/0.15	8.20 ± 1.59	5.44/12.7	0.996 ± 0.002	0.991/0.999
Arruda	Porcine	0.16 ± 1.0	0.05/0.41	1,726 ± 894	267/2,966	0.960 ± 0.030	0.846/0.986
Yeoh	Porcine	0.09 ± 0.06	0.03/0.23	0.01 ± 0.03	−0.04/0.10	0.988 ± 0.004	0.978/0.995
Mooney-Rivlin	Porcine	0.07 ± 0.08	−0.08/0.30	0.01 ± 0.05	−0.06/0.14	0.987 ± 0.004	0.977/0.997

R^2 goodness-of-fit analysis for five common hyperelastic constitutive models derived from human and porcine auricular cartilage stress-strain testing. Max = maximum; Min = minimum; SD = standard deviation.

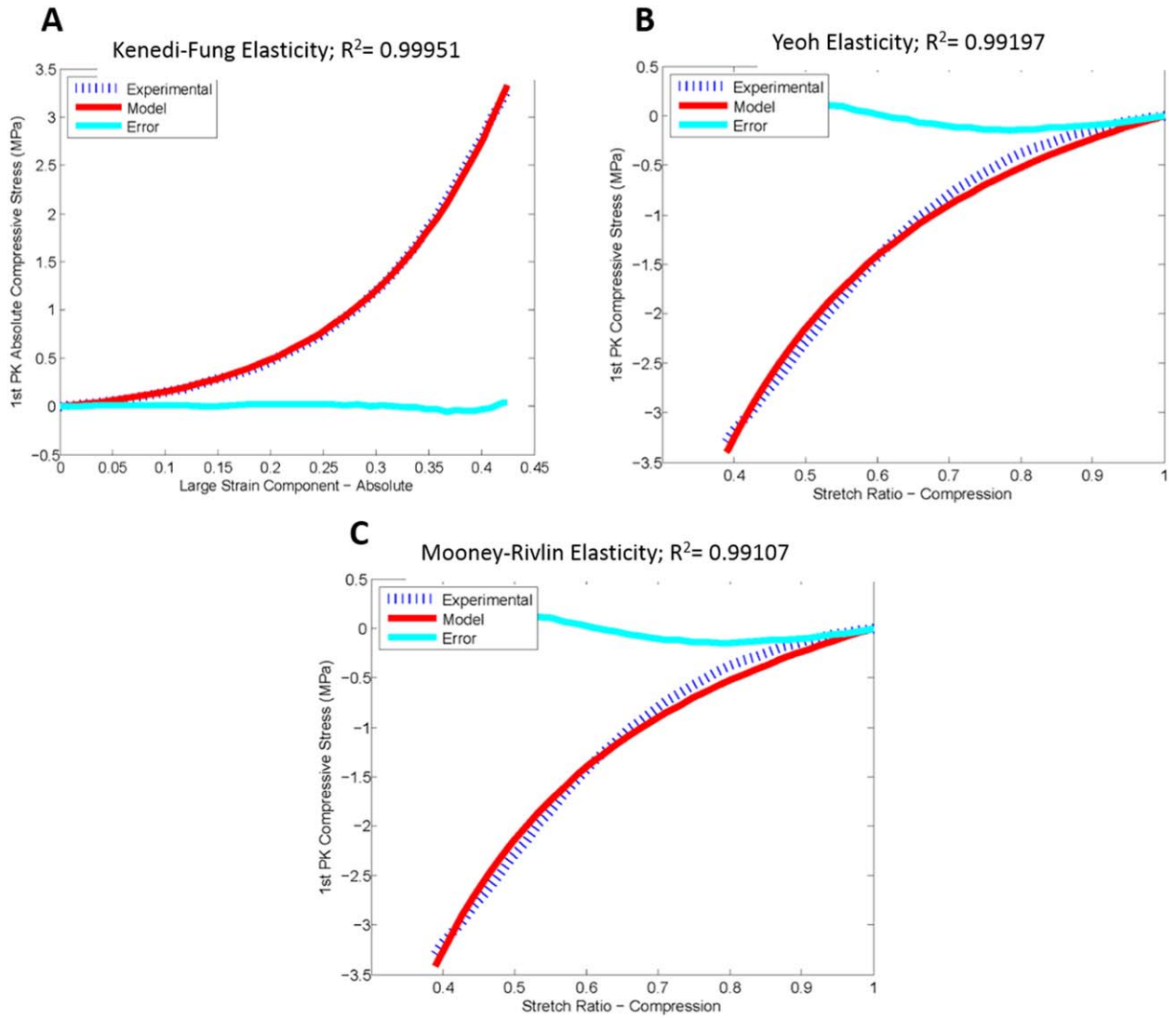

Fig. 4. Graphs of example fits between human ear experimental data (shown by dashed line) and hyperelastic model (solid line) for (A) the Fung/Kenedi model (note Fung/Kenedi model values are shown as absolute values due to the model implementation), (B) the Yeoh model, and (C) the Mooney-Rivlin model.

TABLE III.
Summary of Genetic Phenotypes With Hearing Loss and Cartilaginous Abnormalities.

Phenotype	Location	Genus/Locus	Associated Hearing Loss/Collagen Abnormality
Alport syndrome	Xq22.3	COL4A5	Variable SNHL/collagen IV abnormality
	2q36.3	COL4A3	
Stickler syndrome, type II	1p21.1	COL11A1	High-tone SNHL/collagen X
Osteogenesis imperfecta I	17q21.33	COL1A1	Adolescent onset mixed or CHL/procollagen I
Campomelic dysplasia	17q24.3	SOX9	CHL/collagen II
Spondyloepiphyseal dysplasia	12q13.11	COL2A1	Progressive SNHL/collagen II
Keutel syndrome	12p12.3	MGP	SNHL/abnormal ossification of auricular cartilage

Data were obtained from the Online Mendelian Inheritance in Man database.
CHL = conductive hearing loss; SNHL = sensorineural hearing loss.

porcine and human auricular cartilage. Based on mean R^2 values, the Fung/Kenedi model was the most robust model overall for both porcine and human auricular cartilage biomechanical characteristics. Our analysis also supports the equally valid Yeoh or Mooney-Rivlin constitutive hyperelastic models for use with finite element analysis.

Although the cartilage subtypes present in articular, costal, and nasoseptal cartilage have been extensively characterized, relatively little is known about the biomechanical properties of auricular cartilage. Roy et al.[19] evaluated the use of a large-deflection elasticity model to describe the mechanical behavior of auricular and costal porcine cartilage during three-point bending tests. Their results demonstrated that auricular cartilage has a significantly lower bending modulus than costal cartilage, and also indicated that the orientation of perichondrium in auricular cartilage may influence its mechanical behavior. Most recently, Dahl and colleagues[37] analyzed the biomolecular composition of endogenous auricular cartilage in normal adults, pediatric patients with microtia, and pediatric patients with preauricular appendages. Their immunohistochemical analysis demonstrated similar levels and distribution of elastin and collagens I and X in all three groups of patients, and reduced expression of collagen II in children with microtia. It is likely that this reduction in collagen II expression would lead to changes in mechanical properties, which can be readily characterized using the five nonlinear elastic models tested in this study.

Auricular, septal, and costal cartilage are all frequently utilized in the reconstruction of craniofacial soft tissue defects. Specifically, auricular cartilage autologous grafts are frequently used with a number of surgical approaches including nasal dorsum augmentation and reconstruction, orbital augmentation and floor repair, tarsal plate repair, and stabilization and reconstruction of anterior wall tracheal defects.[38] As described above, available data have demonstrated that auricular cartilage is more flexible than costal and nasoseptal cartilage,[19] yet a comprehensive, objective comparison of the mechanical properties of these cartilage subtypes is limited by a lack of uniform, standardized testing methods. At the present time, the selection of an optimal autologous cartilage source for various surgical scenarios remains in large part dependent on the experience and preference of the reconstructive surgeon, as well as the specific goals of the operation.[39,40]

Our study represents one of the first attempts to define the biomechanical properties of human auricular cartilage. These data help establish a standard by which cartilage autografts, alloplastic implants, and tissue-engineered constructs can be compared in an objective manner. The use of these normative data will be crucial for optimally designing and evaluating proposed implants for auricular reconstruction as well as repair of other defects in the head and neck traditionally repaired using auricular cartilage autografts. The similarity of properties between porcine and cadaveric auricular cartilages supports further use of the pig as a model for microtia research.

Defining robust auricular cartilage mechanical data is also of significant clinical importance in the development of comparative indices for the analysis of genetic defects affecting collagen subtypes that may have phenotypic biomechanical variation of the external cartilaginous auricle. A summary of select genetic syndromes associated with hearing loss and cartilaginous abnormalities are presented in Table III.

A recognized limitation of our study is a lack of experimental data describing the effect of gender or age on the measured biomechanical parameters and behavior of native auricular cartilage.

CONCLUSION

In this study we have presented data characterizing the biomechanical properties of native auricular cartilage, with specific focus on behavior exhibited in response to compressive loading. Auricular cartilage demonstrates nonlinear strain-stiffening elastic behavior that is characteristic of other physiological soft tissues. These auricular cartilage biomechanical data allow for comparative indices in analysis of genetic defects affecting collagen subtypes that may have phenotypic biomechanical variation of the external cartilaginous auricle. In addition, both the whole-ear helix and biopsy compression results provide quantitative targets for designing auricular reconstruction scaffolds. Similarities of the properties between the pig and cadaveric human

auricular cartilage support the use of the pig as a model for microtia reconstruction.

BIBLIOGRAPHY

1. Middlebrooks JC, Green DM. Sound localization by human listeners. *Annu Rev Psychol* 1991;42:135–159.
2. Flint P, Haughey B, Lund V, et al. *Cummings Otolaryngology–Head And Neck Surgery.* 5th ed. Philadelphia, *PA: Mosby Elsevier;* 2010.
3. McGuirt WT, Prasad SD, Griffith AJ, et al. Mutations in COL11A2 cause non-syndromic hearing loss (DFNA13). *Nat Genet* 1999;23:413–419.
4. Donahue LR, Chang B, Mohan S, et al. A missense mutation in the mouse Col2a1 gene causes spondyloepiphyseal dysplasia congenita, hearing loss, and retinoschisis. *J Bone Miner Res* 2003;18:1612–1621.
5. Richards AJ, Fincham GS, McNinch A, et al. Alternative splicing modifies the effect of mutations in COL11A1 and results in recessive type 2 stickler syndrome with profound hearing loss. *J Med Genet* 2013;50:765–771.
6. Brent B. Auricular repair with autogenous rib cartilage grafts: two decades of experience with 600 cases. *Plast Reconstr Surg* 1992;90:355–374.
7. Nagata S. A new method of total reconstruction of the auricle for microtia. *Plast Reconstr Surg* 1993;92:187–201.
8. Romo T, Fozo MS, Sclafani AP. Microtia reconstruction using a porous polyethylene framework. *Facial Plast Surg* 2000;16:15–22.
9. Kamil SH, Kojima K, Vacanti MP, Bonassar LJ, Vacanti CA, Eavey RD. In vitro tissue engineering to generate a human-sized auricle and nasal tip. *Laryngoscope* 2003;113:90–94.
10. Xu J, Johnson TS, Motarjem PM, Peretti GM, Randolph MA, Yaremchuk MJ. Tissue-engineered flexible ear-shaped cartilage. *Plast Reconstr Surg* 2005;115:1633–1641.
11. Rotter N, Steiner A, Scheithauer M. Reconstruction of auricular cartilage using tissue-engineering techniques. *Oper Tech Otolaryngol Head Neck Surg* 2008;19:278–284.
12. Nimeskern L, van Osch G, Müller R, Stok K. Quantitative evaluation of mechanical properties in tissue-engineered auricular cartilage. *Tissue Eng* 2014;20:17–27.
13. Britt JC, Park SS. Autogenous tissue-engineered cartilage: evaluation as an implant material. *Arch Otolaryngol Head Neck Surg* 1998;124:671–677.
14. Ting V, Sims CD, Brecht LE, et al. In vitro prefabrication of human cartilage shapes using fibrin glue and human chondrocytes. *Ann Plast Surg* 1998;40:413–421.
15. Shieh S, Terada S, Vacanti JP. Tissue engineering auricular reconstruction: in vitro and in vivo studies. *Biomaterials* 2004;25:1545–1557.
16. Isogai N, Morotomi T, Hayakawa S, et al. Combined chondrocyte–copolymer implantation with slow release of basic fibroblast growth factor for tissue engineering an auricular cartilage construct. *J Biomed Mater Res A* 2005;74:408–418.
17. Naumann A, Dennis JE, Awadallah A, et al. Immunochemical and mechanical characterization of cartilage subtypes in rabbit. *J Histochem Cytochem* 2002;50:1049–1058.
18. Chang SC, Tobias G, Roy AK, Vacanti CA, Bonassar LJ. Tissue engineering of autologous cartilage for craniofacial reconstruction by injection molding. *Plast Reconstr Surg* 2003;112:793–799.
19. Roy R, Kohles SS, Zaporojan V, et al. Analysis of bending behavior of native and engineered auricular and costal cartilage. *J Biomed Mater Res A* 2004;68:597–602.
20. Mow V. Biphasic creep and stress relaxation of articular cartilage in compression. *J Biomech Eng* 1980;102:73–84.
21. Lee RC, Frank EH, Grodzinsky AJ, Roylance DK. Oscillatory compressional behavior of articular cartilage and its associated electromechanical properties. *J Biomech Eng* 1981;103:280–292.
22. Mak A. The apparent viscoelastic behavior of articular cartilage—the contributions from the intrinsic matrix viscoelasticity and interstitial fluid flows. *J Biomech Eng* 1986;108:123–130.
23. Schinagl RM, Gurskis D, Chen AC, Sah RL. Depth-dependent confined compression modulus of full-thickness bovine articular cartilage. *J Orthop Res* 1997;15:499–506.
24. Schinagl RM, Ting MK, Price JH, Sah RL. Video microscopy to quantitate the inhomogeneous equilibrium strain within articular cartilage during confined compression. *Ann Biomed Eng* 1996;24:500–512.
25. Haisch A, Duda GN, Schroeder D, et al. The morphology and biomechanical characteristics of subcutaneously implanted tissue-engineered human septal cartilage. *Eur Arch Otorhinolaryngol* 2005;262:993–997.
26. Park S, Ateshian GA. Dynamic response of immature bovine articular cartilage in tension and compression, and nonlinear viscoelastic modeling of the tensile response. *J Biomech Eng* 2006;128:623–630.
27. Brown C, Nguyen T, Moody H, Crawford R, Oloyede A. Assessment of common hyperelastic constitutive equations for describing normal and osteoarthritic articular cartilage. *Proc Inst Mech Eng H* 2009;223:643–652.
28. Fung Y. *Biomechanics: Mechanical Properties of Living Tissues*. New York, NY: Springer-Verlag; 1993.
29. Holzapfel G. *Nonlinear Solid Mechanics*. Hoboken, NJ: John Wiley & Sons; 2000.
30. Humphrey JD. *Cardiovascular Solid Mechanics: Cells, Tissues, and Organs*. New York, NY: Springer-Verlag; 2002.
31. Ogden R. Large deformation isotropic elasticity-on the correlation of theory and experiment for incompressible rubberlike solids. *Proc R Soc Lond A Math Phys Sci* 1972;326:565–584.
32. Fung Y. Elasticity of soft tissues in simple elongation. *Am J Physiol* 1967; 213:1532–1544.
33. Yeoh O. Characterization of elastic properties of carbon-black-filled rubber vulcanizates. *Rubber Chem Tech* 1990;63:792–805.
34. Mooney M. A theory of large elastic deformation. *J Appl Phys* 1940;11: 582–592.
35. Rivlin R. Large elastic deformations of isotropic materials. IV. Further developments of the general theory. *Phil Trans Roy Soc Lond A* 1948; 241:379–397.
36. Arruda EM, Boyce MC. A three-dimensional constitutive model for the large stretch behavior of rubber elastic materials. *J Mech Phys Solids* 1993;41:389–412.
37. Dahl JP, Caballero M, Pappa AK, Madan G, Shockley WW, van Aalst JA. Analysis of human auricular cartilage to guide tissue-engineered nanofiber-based chondrogenesis: implications for microtia reconstruction. *Otolaryngol Head Neck Surg* 2011;145:915–923.
38. Tardy ME, Denneny J, Fritsch MH. The versatile cartilage autograft in reconstruction of the nose and face. *Laryngoscope* 1985;95:523–533.
39. Porter JP. Grafts in rhinoplasty: alloplastic vs autogenous. *Arch Otolaryngol Head Neck Surg* 2000;126:558–561.
40. Toriumi DM. Autogenous grafts are worth the extra time. *Arch Otolaryngol Head Neck Surg* 2000;126:562–564.